

Electrophoresis of a Rod Macroion under Polyelectrolyte Salt: Is Mobility Reversed for DNA?

Motohiko Tanaka §

National Institute for Fusion Science, Toki 509-5292, Japan

Abstract. By molecular dynamics simulation, we study the charge inversion phenomenon of a rod macroion in the presence of polyelectrolyte counterions. We simulate electrophoresis of the macroion under an applied electric field. When both counterions and coions are polyelectrolytes, charge inversion occurs if the line charge density of the counterions is larger than that of the coions. For the macroion of surface charge density equal to that of the DNA, the reversed mobility is realized either with adsorption of the multivalent counterion polyelectrolyte or the combination of electrostatics and other mechanisms including the short-range attraction potential or the mechanical twining of polyelectrolyte around the rod axis.

1. Introduction

The charge inversion phenomenon takes place due to strong correlations of a macroion with small salt ions in solution, which has recently been studied for the physiochemical and bio-engineering systems [1, 2, 3, 4, 5, 6, 7, 8, 9, 10, 11, 12, 13, 14]. Of particular interest is its possibility of facilitating the delivery of genes through negative cell walls [15, 16]. In our previous studies by molecular dynamics simulations [9, 10], we adopted both static and dynamic models for the macroions. Specifically, in the dynamical study of electrophoresis with explicit (particle) solvent [10], we directly proved the charge inversion by measuring the drift of the macroion along the external electric field. The net charge of the macroion complex was estimated with the use of the force balance $Q^* \sim \nu\mu$, where μ is the electrophoretic mobility and ν is the solvent friction.

The purpose of this paper is to demonstrate the possibility of mobility reversal under electrophoresis, as the result of charge inversion, for elongated macroions including the DNA. Simulation method and parameters are summarized below. We take the system of one macroion, many counterions, coions and neutral particles as solvent. The units of length, charge and mass are, a , e , and m , respectively ($a \sim 1.4\text{\AA}$ in water and $m \sim 40$ a.m.u.) The rod is assumed to lie perpendicularly to the applied electric field which extends fully across the periodic system. It was shown that a finite-length rod rotates and aligns parallel to the electric field due to the rod polarization by specific condensation of positive ions at one end toward the electric field and the negative ions at the other end [5, 17]. Charge inversion occurs similarly in that case, but the discreteness of the surface charge is essential since the counterions need to be pinned down on the smooth surface of the rod macroion [17].

§ Email address: mtanaka@nifs.ac.jp

The macroion has a radius $R_0 = 5a$, negative charge Q_0 with $-20e$ or $-80e$, and mass $2000m$, which is surrounded by the N^+ number of counterions of a positive charge Z^+e and the N^- coions of a negative charge $-Z^-e$. The system is maintained in overall charge neutrality, $Q_0 + N^+Z^+e - N^-Z^-e = 0$. The radii of counterions and coions are a^+ and a^- , respectively, with the counterion radius being fixed $a^+ = a$, and that of neutral particles is $a/2$. The mass of the coions and counterions is m , and that of N_* neutral particles is $m/2$. Approximately one neutral particle is distributed in every volume element $(2.1a)^3 \approx (3\text{\AA})^3$ inside the periodic simulation domain of the side $L = 32a \approx 45\text{\AA}$, excluding the locations already occupied by ions.

We solve the Newton equations of motion for each particle with the electrostatic (Coulombic) and Lennard-Jones potential forces under the uniform applied electric field E ($E > 0$). A large number of neutral particles are used to model the viscous solvent of given temperature and to treat the interactions among the finite-size macroion, counterions, coions and solvent. The Coulombic forces under the periodic boundary conditions [18] are calculated efficiently with the use of the so-called particle-particle-particle-mesh algorithm [19, 20], with $(32)^3$ spatial meshes, the real-space cutoff $10a$ and the Ewald parameter $\alpha \approx 0.262$ (the electric field is accurately calculated with the Ewald method). The volume exclusion effects between particles (both charged and non-charged) are treated with the repulsive Lennard-Jones potential $\phi_{LJ} = 4\varepsilon[(A/r_{ij})^{12} - (A/r_{ij})^6]$ for $r_{ij} = |\mathbf{r}_i - \mathbf{r}_j| \leq 2^{1/6}A$, and $\phi_{LJ} = -\varepsilon$ otherwise. Here \mathbf{r}_i is the position vector of the i -th particle, and A is the sum of the radii of two interacting particles. We relate ε with the temperature by $\varepsilon = k_B T$, and choose $k_B T = e^2/5\epsilon a$ (we assume spatially homogeneous dielectric constant ϵ). The Bjerrum length is thus $\lambda_B = e^2/\epsilon k_B T = 5a$, which is 7\AA in water. The equations of motion are integrated with the use of the leapfrog method, which is equivalent to the Verlet algorithm [21]. The unit of time is $\tau = a\sqrt{m/\varepsilon}$ ($\approx 1\text{ps}$), and we choose the integration time step $\Delta t = 0.01\tau$.

The Joule heat produced by the external electric field on ions and transferred to neutral particles by collisions is drained by a heat bath for neutral particles at the boundaries. The thermal bath which screens hydrodynamic interactions is safely adopted in the present study since the hydrodynamic interactions are screened at short distances in the electrolyte solvent [22, 23]. We confirmed this fact by good agreement of our results with and without the heat bath [10]. We also note that the effects of finite length and rotation of the rod macroion were discussed in [17, 24].

2. A Rod Macroion with Polyelectrolytes

2.1. Polyelectrolyte Counterions and Coions

We showed previously that the mobility of a rod (cylindrical) macroion reversed its sign at zero salt, which was enhanced by addition of small amount of monovalent salt if the macroion was strongly charged, $\sigma_{rod} = |Q_{rod}|/2\pi R_{rod}L > 0.04e/a^2$ (0.33 C/m^2) [24]. For reference, the surface charge density of the DNA is 0.19 C/m^2 . The reversed mobility of the rod macroion was more persistent to larger amount of monovalent salt than the spherical macroion of the same radius and surface charge density. However, the rod macroion with surface charge density equal to that of the DNA was not subject to mobility reversal. As will be shown in this paper, polyelectrolyte counterions can promote overcharging of the macroion [25].

Figure 1 shows the charge inversion of a rod macroion when both the counterions

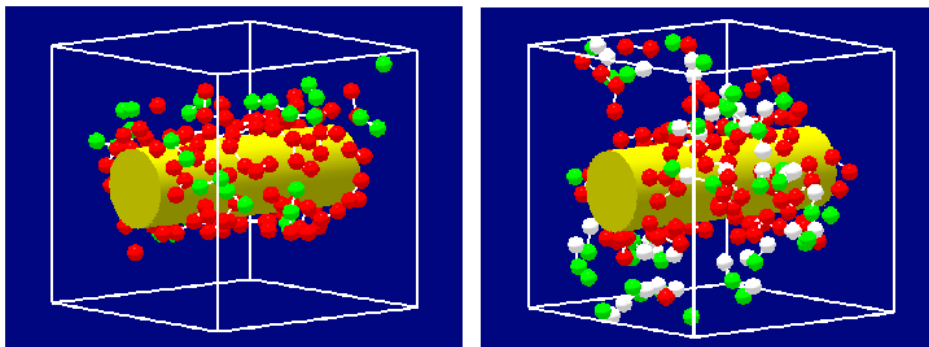


Figure 1. The rod-shaped macroion under polyelectrolyte counterions and coions. All chains consist of four monomers; each of 30 counterion polyelectrolyte chains carries four unit charges e (red monomers). The coion polyelectrolyte is either (left) 10 chains consisting of four unit charges ($-e$) (green monomers), or (right) 20 chains of two unit charges and two neutral monomers (white monomers).

Table 1. The mobility of the infinite rod macroion $Q_{rod} = -80e$ under polyelectrolyte counterions and coions. Among 30 counterion polyelectrolyte chains consisting of four unit charges e , 20 chains are required to neutralize the macroion. The line charge density of the coion polyelectrolyte is varied, where each chain consists of one, two or four unit charges ($-e$) and interleaving neutral monomers for the rest. Also, the case with monovalent salt, $N_{salt}^+ = 80$ and $N_{salt}^- = 80$ is shown in the bottom row. The mobility values are in unit of $10^{-2}\mu_{0r}$.

charges \times chains	$-4e \times 10$	$-2e \times 20$	$-e \times 40$
no salt	1.3	3.2	3.4
w/ salt	-4.9	-0.085	-0.36

and coions are polyelectrolytes. For simplicity, all chains have the same length of four monomers. All the monomers are charged unity e for 30 chains of counterion polyelectrolyte (red monomers). For the coions, there are two cases: (a) 10 chains of four unit charges ($-e$) (green monomers), and (b) 20 chains, each consisting of two unit charges ($-e$) and two neutral monomers (white). When the line charge densities of the counterion and coion polyelectrolytes are equal as in Fig.1(a), the mobility reversal is small as shown in Table I (the bin of $-4e \times 10$ and "no salt"). This is because the well adsorbed coion polyelectrolyte cancel charges of the counterion polyelectrolyte. When the line charge density of the coion polyelectrolyte is reduced to a half, adsorption of coion polyelectrolyte becomes less as shown in Fig.1(b), and significant reversed mobility is obtained (the bin of $-2e \times 20$ and "no salt"). Further reduction of the line charge density of coion polyelectrolyte yields nearly the same reversed mobility. When the monovalent salt whose charge content is twice as large as that of the coion polyelectrolyte is added, the mobility of the macroion is non-reversed (the bottom row of Table I). Charge neutralization by the coion polyelectrolyte is good when its line charge density is comparable to that of the counterion polyelectrolyte.

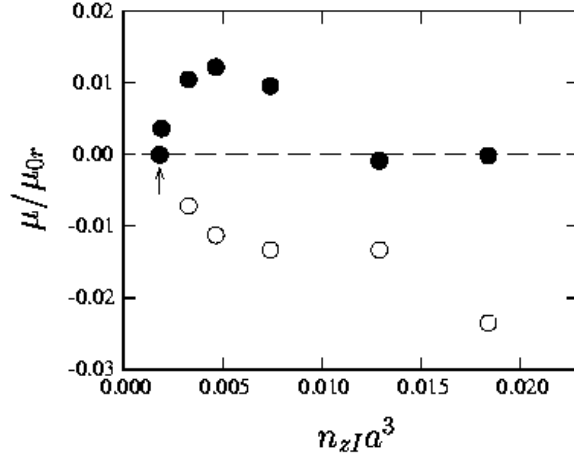


Figure 2. The mobility of a cylindrical macroion against the ionic strength of polyelectrolyte counterions $n_{zI} = Z^2N^+/L^3$, where $\mu_{0r} \approx 2.8 \times 10^{-4}$ (cm/s)/(V/cm) and $0.005e/a^3 \approx 0.33$ M/l. Unit charges placed along double helices provide the macroion surface charge with $\sigma_{rod} \approx 0.02e/a^2$ (0.17 C/m² $\sim \sigma_{DNA}$). (a) Each counterion chain consists of three trivalent Z-ions (filled circles), (b) the same as (a) except that all counterions are isolated spheres (open circles). The coions are larger than the counterions $a^-/a^+ = 1.5$. The arrow shows the isoelectric point.

2.2. A Rod Macroion with Surface Charge Density Equal to the DNA

Previous studies of charge-inverted rod macroions (polyelectrolyte) dealt with their condensation to a charged surface [5, 6, 7], or the adsorption of metal ions on themselves [1] except for a very recent study [26]. Here, we treat the charge inversion of a cylindrical macroion in the presence of polyelectrolyte counterions, where the surface charge density of the macroion is approximately that of the DNA, $\sigma_{rod} \approx 0.02e/a^2$. The macroion is assumed to be an infinite rod with $Q_{rod} = -20e$, radius $R_{rod} = 5a$ and mass $2000m$, lying perpendicularly to the applied electric field. The surface charges are provided by two sets of ten discrete charges ($-e$) aligned helically at the depth a below the surface of the rod; the spacing of unit charges is $4.1a$ along the helix contour. The polymer counterions (polyelectrolyte) consist of the monomers either of (i) trivalent ions or (ii) monovalent ions. The coions are monovalent with larger radius than the counterions $a^-/a^+ = 1.5$, which is favorable for charge inversion [24]. The Bjerrum length is $e^2/\epsilon k_B T = 5a$. The mobility normalization is $\mu_{0r} = v_0/(2|Q_{rod}|/R_{rod}L) = v_0/4\pi\sigma_{rod} \approx 2.8 \times 10^{-4}$ (cm/s)/(V/cm), where v_0 is the thermal speed of neutral particles. The Z-ion concentration at $n_{zI} \approx 0.005/a^3$ is approximately 0.33 M/l.

For the counterion polyelectrolyte with $3e - 3e - 3e$ monomers, the macroion mobility is reversed as denoted by filled circles in Fig.2. The reversed mobility increases with the ionic strength of Z-ions as $n_{zI}^{1/2}$ above the isoelectric point (arrow), as predicted by theory [7]. Then, the mobility decreases and gets non-reversed since more coions condense on the counterion polyelectrolyte as the number of screening coions increases with the ionic strength. This is verified in the radial distribution functions in Fig.3, where the profile of the integrated charge for the large ionic strength in Fig.3(b) has an overshoot and is less prominent. This overshoot is characteristic of non-reversed

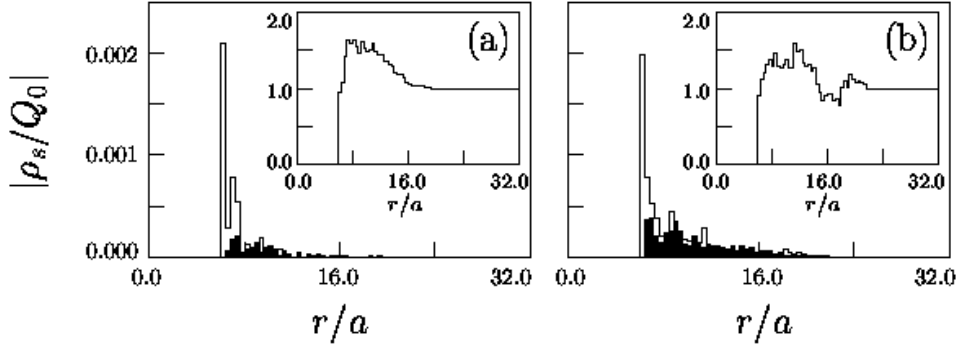


Figure 3. The distribution functions of the counterions (open bars) and coions (shaded bars) for the rod macroion with double helix charges whose surface charge is equal to that of the DNA. These correspond to the filled circles in Fig.2 with the ionic strength (a) $n_{zI} \sim 0.005a^{-3}$ and (b) $n_{zI} \sim 0.013a^{-3}$.

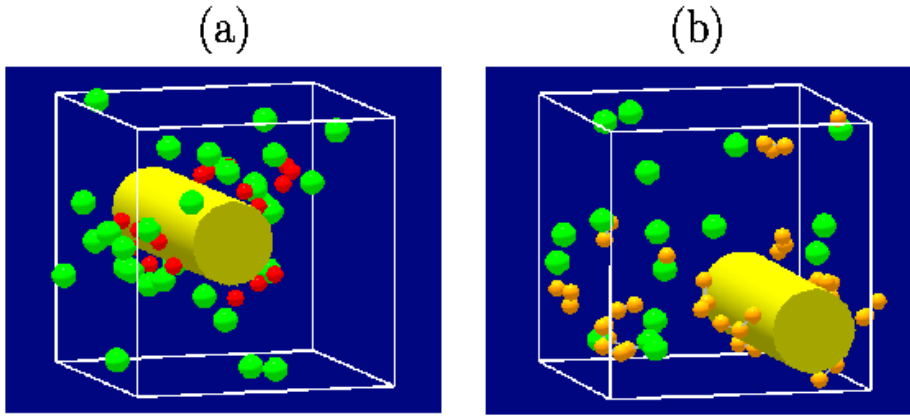


Figure 4. A rod macroion whose surface charges are provided by discrete unit charges along double helices with the surface charge density nearly equal to that of the DNA, is shown for (a) polyelectrolyte cations of three trivalent ions $N^{+3} = 17$ (red spheres), and (b) polyelectrolyte of three monovalent ions $N^{+} = 35$ (yellow spheres). The former corresponds to the filled circle in Fig.2 at $n_{zI} \sim 0.005/a^3$. The anions (green spheres) are larger than the cations, $a^-/a^+ = 1.5$. The external electric field points horizontally rightward.

mobility in spite of the peaked charge profile [24]. At the point where the reversed mobility terminates, the charge content of the salt in the surface layer is still less than that of the macroion surface charge, $Zec_s\lambda_D \sim \frac{1}{4}\sigma_{rod}$. Good adsorption of the polyelectrolyte Z-ions is seen in the bird's-eye view plot of Fig.4(a), where the average bond length between the chained Z-ions is $3.2a$. This behavior agrees with the result of the theory [27]. Also, it may be related to the electrophoresis experiment that observed reversed mobility for the concentration ratio of [polycation]/[DNA] ≈ 2 , where the macroion was a chicken embryo DNA and the polycation was monovalent polymer with a long hydrophobic chain $(CH_2)_nCH(C_5NH_4)^+C_2H_5$ [28]. The differences of the experiment from the simulation setting, however, are the monovalence and existence of the hydrophobic chain, which will be mentioned in the next subsection.

For isolated Z-ions with other conditions fixed as above, the mobility reversal does not occur (open circles in Fig.2). The counterion condensation is weak in this case, possibly due to desorption of counterions by thermal agitation. The correlation energy between the surface Z-ions, calculated with the Wigner-Seitz cell radius $R_{WS} = (Z/\pi\sigma_{rod})^{1/2} \sim 6.9a$,

$$Z^2e^2/2\epsilon R_{WS} \sim 3.3k_B T \quad (1)$$

is comparable to thermal energy, which is below the threshold of charge inversion. Thus, the polyelectrolyte counterions with a rod macroion is more favorable for the mobility reversal than with the isolated counterions for the same ionic strength [17].

For a strongly charged rod macroion with $\sigma_{rod} \sim 0.08e/a^2$, the mobility is reversed and increases above the isoelectric point. The peak mobility occurs around $n_{zI} \sim 0.02a^{-3}$ with $\mu \sim 0.04\mu_{0r}$. The Z-ion correlation energy here is twice large compared to the previous case, $Z^2e^2/2\epsilon R_{WS} \sim 6.5k_B T$ ($R_{WS} \sim 3.5a$). The reversed mobility, i.e. net overcharging, increases in proportion to the macroion bare charge. The theory of an infinite-length rod adsorption on a two dimensional plane can be applied to the present simulation if one makes the following replacements, the DNA \rightarrow polyelectrolyte, the planar surface \rightarrow the rod macroion, which predicts net overcharging [5, 7]

$$Q^* \sim (\eta/\lambda_D)/\ln(\eta/\sigma_{rod}\lambda_D). \quad (2)$$

Here, the line charge density of the polyelectrolyte $\eta \sim e/3.2a$ predicts 2.6 times more overcharging for the strongly charged macroion than the weakly charged macroion. Our result agrees well with the theory prediction.

As the second case, the electrophoresis of the same macroion under all unit-charge polyelectrolyte is examined. The short polyelectrolyte whose charge content (chain length) is less than $10e$ is not subject to charge inversion. The electrostatic energy between the unit charges with the mutual distance $b \sim 3a$ is $e^2/\epsilon b \sim \frac{5}{3}k_B T$. Although the Manning-Onsager condensation of coions [29] on the counterion polyelectrolyte is not evident in Fig.4(b), the adsorption of such polyelectrolyte is not as strong as to cause charge inversion. The radial distribution function and the bird's-eye view plot of Fig.4(b) reveal that about a half of such polyelectrolyte chains are located away from the macroion surface, thus the net charge of the macroion complex is negative. It is mentioned in passing that the present molecular dynamics simulation is not reproducing the charge inversion due to optimal adsorption of unit-charge polyelectrolyte through fractionalization [30].

2.3. Non-Electrostatic Mechanisms for Mobility Reversal

As mentioned above, the unit-charge polyelectrolyte of reasonable length alone does not lead to mobility reversal. Nevertheless, we show below that the mobility reversal occurs for such polyelectrolytes if another mechanism is superimposed. For example, the polymers with hydrophobic tails feel short-range attraction forces around the DNA. Here, this effect is modeled with the attractive Lennard-Jones potential of the depth $1k_B T$, without truncation of the potential at the distance $2^{1/6}\sigma$. A reversed mobility is obtained for the polyelectrolyte counterions of 10 unit charges, $\mu \approx 0.015\mu_{0r}$. An analytical theory showed reversed mobility for the surfactant having a charged head group and hydrophobic tails with strong hydrophobicity $\chi = -6k_B T$ [25]. Our molecular dynamics simulation uses a weak attraction potential but requires rather a

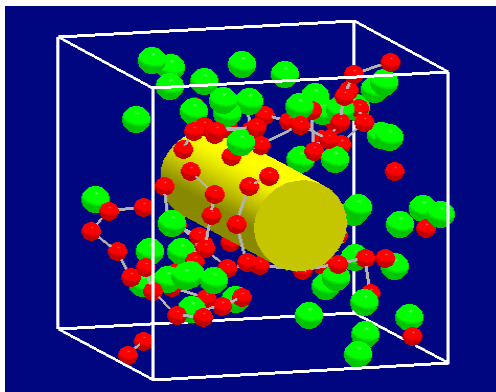


Figure 5. A cylindrical macroion with long polyelectrolyte cations of unit charges (red) and isolated anions (green) has reversed mobility. The surface charge density of the macroion with double helix charges, $\sigma_{rod} \sim 0.02e/a^2$, is approximately that of the DNA. The long chains of polyelectrolyte mechanically wind around the rod. The radius and number of anions are $a^- = 1.5a$ and $N^- = 60$, respectively [neutral particles are not shown].

long chain. More works are necessary to reconcile these results with the experiment using the DNA as the macroion and monovalent counterion polyelectrolyte [28].

The following simulation result gives an implication where large reversed mobility $\mu \approx 0.073\mu_0$ occurs for a very long polyelectrolyte chain of $20e$. This mobility reversal is due to mechanical twining of the polyelectrolyte chain around the rod axis, as depicted in Fig.5. These chains are not statically attached to the macroion, but they pull the macroion by twining toward the electric field on time average. However, when the chain length is cut to a half with the total number of counterions fixed, mobility is not reversed as the chains can pass by the rod. Although the mechanical twining of polyelectrolyte counterions is not due to electrostatics, both the electrostatic and non-electrostatic mechanisms can work together to cause the mobility reversal of the DNA macroion in the electrophoresis experiments.

3. Summary

In this paper, the charge inversion phenomenon of a rod macroion under polyelectrolyte counterions was studied. When both the counterions and coions were polyelectrolytes, the charge inversion took place if the line charge density of the counterions prevailed over that of coions. The mobility was reversed for the rod macroion of the surface charge density equal to that of the DNA due to polyelectrolyte counterions of multi-valence.

For short chains of counterion polyelectrolyte consisting of unit charges, the electrostatic effect alone was not sufficient to cause mobility reversal. Either the short-range attraction due to hydrophobicity or the mechanical twining of the polyelectrolyte around the rod macroion could cause the mobility reversal. In real environments, the electrostatic mechanism and other effects such as hydrophobic attraction by specific configurations or mechanical twining of the polyelectrolytes may collaborate to result

in the mobility reversal under the electrophoresis.

Acknowledgments

The author cordially thanks Prof.A.Yu.Grosberg for close collaborations on the molecular dynamics study of the charge inversion phenomenon. This study and the travel to participate in *The International Conference of Applied Statistical Physics of Molecular Engineering 2003* (Mexico) was supported by Grant in Aid No.15035218 (2003) from the Ministry of Education, Science and Culture of Japan. The computation was performed with the computers of the University of Minnesota Supercomputing Institute, and those of the Institute for Space and Astronautical Science of Japan.

- [1] E.Gonzalez-Tovar, M.Lozada-Cassou, and D.J. Henderson, *J. Chem.Phys.* **83**, 361 (1985).
- [2] H.W.Walker and S.B.Grant, *Colloids Surfaces A119*, 229 (1996).
- [3] V.A.Bloomfield, *Biopoly.* **44**, 269 (1998).
- [4] H.Greberg, and R.Kjellander, *J.Chem.Phys.* **108**, 2940 (1998).
- [5] R.R.Netz and J.F.Joanny, *Macromolecules* **32**, 9013 (1999).
- [6] W.R.Gelbart, R.Bruinsma, P.Pincus and A.Parsegian, *Physics Today* **53**, 38 (2000).
- [7] T.T.Nguyen, A.Yu. Grosberg and B.I. Shklovskii, *Phys. Rev. Lett.* **85**, 1568 (2000).
- [8] R.Messina, C.Holm and K.Kremer, *Phys.Rev.Lett.* **85**, 872 (2000).
- [9] M.Tanaka and A.Yu. Grosberg, *J.Chem.Phys.* **115**, 567 (2001).
- [10] M.Tanaka and A.Yu. Grosberg, *Euro.Phys.J., E7*, 371 (2002).
- [11] M.Lozada-Cassou, E.Gonzalez-Tovar, and W.Olivares, *Phys.Rev. E* **60**, R17 (1999); M.Lozada-Cassou and E.Gonzalez-Tovar, *J.Colloid Interf.Sci.* **239**, 285 (2001).
- [12] A.Yu. Grosberg, T.T. Nguyen, and B.I. Shklovskii, *Reviews Modern Phys.*, **74**, 329 (2002).
- [13] Y.Levin, *Rep.Prog.Phys.* **65**, 1577 (2002).
- [14] M.Quesada-Perez, E.Gonzalez-Tovar, A.Martin-Molina, M.Lozada-Cassou, and R.Hidalgo-Alvarez, *ChemPhysChem.* **4**, 234 (2003).
- [15] A.V.Kabanov, V.A.Kabanov, *Bioconj.Chem.*, **6**, 7 (1995).
- [16] K.Ewert, A.Ahmad, H.M.Evans, H.W.Schmidt, and C.R.Safinya, *J.Med.Chem.*, **45**, 5023 (2002).
- [17] M.Tanaka, *Slow Dynamics in Complex Systems* (edited by M.Tokuyama and I.Oppenheim, AIP Conference Series, 2004).
- [18] P.P.Ewald, *Ann.Physik* **64**, (1921) 253.
- [19] J.W.Eastwood and R.W.Hockney, *J.Comput.Phys.* **16**, (1974) 342.
- [20] M.Deserno and C.Holm, *J.Chem.Phys.* **109**, (1998) 7678.
- [21] D.Frenkel and B.Smit, *Understanding Molecular Simulation* (Academic Press, 1996)
- [22] D.Long, J.-L.Viovy, and A.Ajdari, *Phys.Rev.Lett.*, **76**, 3858 (1996).
- [23] J.-L.Viovy, *Rev.Mod.Phys.* **72**, (2000) 813.
- [24] M.Tanaka, *Phys.Rev.E*, **68**, 061501 (2003).
- [25] M.B.A.Silva, P.S.Kuhn and L.S.Lucena, *Physica A296*, 31 (2001).
- [26] R.Messina, *J.Chem.Phys.*, **119**, 8133 (2003).
- [27] T.T.Nguyen and B.I. Shklovskii, *J.Chem.Phys.* **114**, 5905 (2001).
- [28] S.A.Sukhishvili, O.L.Obolskii, L.V.Astafieva, A.V.Kabanov, and A.A.Yaroslavov, *Vysokomol.Soed.* **35**, 1895 (1993) [*Polymer Sci. A35*, 1602 (1993).]
- [29] G.J.Manning, *J.Chem.Phys.* **51**, 924 (1969).
- [30] T.T.Nguyen and B.I. Shklovskii, *Phys.Rev.Lett.*, 018101 (2002).